Mine Countermeasures & Demining Conference, Asia-Pacific Issues & MCM in Wet Environments, 9-11 February 2004, Canberra, Australia

Dynamics of bottom mine burial in soft sediments: experimental evidence and predictions

By

A.V. Abelev, P.J. Valent,

Naval Research Lab,
Bldg. 1005,
Stennis Space Center, MS 39529, USA
Tel. 228-688-4650
Fax. 228-688-4093
Emails:
Andrei.Abelev@nrlssc.navy.mil
Phil.Valent@nrlssc.navy.mil

Abstract

The paper presents results of 21 deployments of an instrumented, mine-like cylinder over soft cohesive sediment seafloor at two sites. The focus of this work is the sediment penetration phase. The paper gives a statistical description of the sediment penetration dynamics and compares the observed behavior with predictions from an impact burial software package. It is shown that, due to simplifications and assumptions adopted in the package, the predictions are only marginally acceptable in describing the experimentally observed motions, orientations and amount of burial. It is further shown that extending the currently two-dimensional formulation of the predictive software may not result in significant improvements of the overall predictions of impact burial. It is argued that such improvements may only be achieved through a more accurate constitutive model of the deforming sediment.

Introduction

The main objective of this study is to collect, systematically analyze, and quantify the experimental data on the complex three-dimensional behavior of an instrumented cylinder during freefall and penetration into the sediment floor. The experimental results are compared with the model predictions, utilizing the state-of-the-art software package. This information is relevant to the implementation of the mine burial procedures, calculating the amount of burial of a potential mine in the seafloor marine sediments, and depends on our knowledge of the two main categories of data. One consists of the accurate description of the characteristics of the bottom sediments, pertaining to the high strain and high strain rate deformation. This knowledge also needs to reflect the natural variability of these parameters in both spatial and temporal domains. Information on the linear and angular velocities and orientation of the falling mine at the point of

REPORT DOCUMENTATION PAGE

Form Approved
OMB No. 0704-0188

1. REPORT DATE *(DD-MM-YYYY)*
02-OCT-2003

2. REPORT TYPE
Conference Proceedings, (not refereed)

3. DATES COVERED *(From - To)*

4. TITLE AND SUBTITLE
Dynamics of Bottom Mine Burial in Soft Sediments: Experimental Evidence and Prediction

5a. CONTRACT NUMBER

5b. GRANT NUMBER

5c. PROGRAM ELEMENT NUMBER
62435N

6. AUTHOR(S)
Andrei V Abelev PHILIP J VALENT

5d. PROJECT NUMBER
BE-782-001

5e. TASK NUMBER

5f. WORK UNIT NUMBER

7. PERFORMING ORGANIZATION NAME(S) AND ADDRESS(ES)
Naval Research Laboratory
Marine Geoscience Division
Stennis Space Center, MS 39529-5004

8. REPORTING ORGANIZATION REPORT NUMBER
NRL/PP/7400--03-3

9. SPONSORING/MONITORING AGENCY NAME(S) AND ADDRESS(ES)
Office of Naval Research
Ballston Centre Tower One
800 North Quincy Street
Arlington VA 22217-5660

10. SPONSOR/MONITOR'S ACRONYM(S)
ONR

11. SPONSOR/MONITOR'S REPORT NUMBER(S)

12. DISTRIBUTION/AVAILABILITY STATEMENT
Approved for public release,distribution is unlimited Approved for public release, distribution unlimited

13. SUPPLEMENTARY NOTES

14. ABSTRACT
The paper presents results of 21 deployments of an instrumented, mine-like cylinder over soft cohesive sediment seafloor at two sites. The focus of this work is the sediment penetration phase. The paper gives a statistical description of the sediment penetration dynamics and compares the observed behavior with predictions from an impact burial software package. It is shown that, due to simplifications and assumptions adopted in the package, the predictions are only marginally acceptable in describing the experimentally observed motions, orientations and amount of burial. It is further shown that extending the currently two-dimensional formulation of the predictive software may not result in significant improvements of the overall predictions of impact burial. It is argued that such improvements may only be achieved through a more accurate constitutive model of the deforming sediment.

15. SUBJECT TERMS
mine-like cylinder, seafloor, impact burial, two-dimensional

16. SECURITY CLASSIFICATION OF: a. REPORT	b. ABSTRACT	c. THIS PAGE	17. LIMITATION OF ABSTRACT	18. NUMBER OF PAGES	19a. NAME OF RESPONSIBLE PERSON
					PHILIP J. VALENT
					19b. TELEPHONE NUMBER *(Include area code)*
Unclassified	Unclassified	Unclassified	UL		228-688-4650

Standard Form 298 (Rev. 8/98)

impact on the sediment floor represents the second class of the input information required for the penetration burial prediction.

Behavior of cylindrical bodies during free-fall through the water column has been modeled in the past [1] and [2]. Further developments are underway, involving improved and more realistic approaches, e.g. [3]. The amount of knowledge available for modeling of the penetration into soft cohesive seafloor sediments, however, is rather limited. Both material description and computational scheme are crude and do not address several important phenomena and processes typical to soft sediments. These phenomena include the effects of the high strains and strain rates on sediment resistance to penetration, as well as issues related to inherent sediment heterogeneity of physical properties.

The goal of this paper is to present the results of two series of experimental deployments of a full scale instrumented cylinder, released in a realistic field setting. The two series of tests include deployments off the coast of Corpus Christi, TX (test ID: "G06") and off the coast of Cocodrie, LA (test ID "P02") performed in January and May of 2002, respectively. The instrument data is used to characterize the dynamic behavior exhibited by this cylinder. In the next section (Experimental Setup) we describe the instrumented cylinder and its deployment. Then, we present the statistical characterization of the observational results and comparisons with theoretical predictions. Further, the effects of the reduced dimensionality of the problem in the model are addressed through experimental observations. Our findings are summarized in the conclusion section.

Experimental setup equipment, and procedures

Instrumented cylinder and data acquisition

The instrumented cylinder measures 0.53 m in diameter and 2.40 m long, yielding a length to diameter ratio of 4.5. Its weight in air is approximately 10 kN (2250 lb) and its weight in water (seawater) is about 4.9 kN. Most bottom mines of the type considered here are slightly nose heavy, and so the instrumented cylinder designed for this study had the distance between the center of mass (CM) and the center of volume (CV) of 0.104 m, with the CM located forward of the CV. Three different and interchangeable nose shapes were manufactured: blunt, hemispherical, and chamfered, again representing a variety of operational mines. Fig. 1 depicts the instrumented cylindrical shape, strapped to a cradle and with the blunt nose mounted.

The internal instrumentation, placed in the sealed container inside the cylinder, included a set of accelerometers measuring along three orthogonal axes. These accelerometers had three different ranges: 2.5g, 4g, and 10g. Additionally, a tri-axial fiber-optic gyro (FOG) measured the angular rotation rate about three orthogonal axes, collinear with the axes of the accelerometer. A tri-axial magnetometer was also placed inside the instrumentation chamber. Interpretation of its measurements, however, was not implemented due to the difficulties in calibration. The internal instrumentation also included a power source, a signal acquisition and conditioning unit, and a fast access memory storage device.

An upgraded and expanded version of the data processing software, originally reported in [4], was developed. The raw device data, which included variations of the components of local (cylinder's coordinate system) accelerations and angular rotation rates with time was analyzed.

First, the transformation was performed from the local (cylinder) coordinate system to the fixed global system, using the Euler aerospace rotation sequence. The effects of gravity were then removed and the resulting values of accelerations and angular rotation rates were integrated to obtain a set of global (in addition to local) velocities, displacements, and angular changes as functions of elapsed time. Processing from its initial state, with the cylinder suspended from the ship's winch, forward proved somewhat ambiguous and was replaced with the reversed integration from the cylinder's final position at rest, embedded in the sediment, backwards. The advantage of this approach was in the fact that the conditions at rest are easier and more accurately defined than those at the time of release. Comparisons between the forward and reverse integration schemes showed only minor errors in the overall calculated displacements, accumulated over the entire trajectory.

The data post-processing routines resulted in a set of data that allows analysis of many individual components of the process of free fall and penetration into the sediment. Fig. 2 represents an example of a typical visualization of the calculated trajectory of the cylinder during free fall. Accurate and detailed analysis of various components of acceleration also allowed for estimating the initial point of contact of the cylinder with the sediment floor. This point was typically characterized by a sharp spike in one or more components of the acceleration and angular rotation rates. The details of this determination are presented below. Accurate separation between the trajectory in the water and penetration into the sediment is essential for appropriate comparisons with predicted data.

Testing procedures

The data reported in this study was obtained during two cruises. These cruises included the January 2002 cruise on board R/V Pelican, in the vicinity of Cocodrie, LA and the May 2002 cruise on board R/V Gyre, in the vicinity of Corpus Christi, TX.

Each of the two trips included a series of drops with varying cylinder nose configurations and initial conditions. Only one nose configuration was used during the Cocodrie trip, while the cylinder with all three noses was tested during the Corpus Christi trip. Release medium was also varied with some of the cylinder deployments performed from the air, usually only a small height above the water surface, and some others released from the fully submerged position of just below the water surface. Additionally, the initial inclination (pitch) was changed by using different strapping. Two configurations were tested: horizontal and at 31 degrees nose down. Table 1 summarizes this information, showing the test name designations, and the release conditions. Test numbers, referred to hereafter, follow the sequential numbering order, given in the first column of the table.

The testing sequence proceeded according to the following order. First the internal instrumentation of the cylinder resting in its cradle was initialized. The cylinder was then suspended by either the harness or from the bomb release (as shown in Fig. 3), brought to the desired elevation above or below the water surface and released. A ¼" line was attached to the cylinder and trailed it to the bottom. This line was necessary for the subsequent location and recovery of the cylinder due to almost zero visibility encountered in both deployment areas. The divers then followed this line to the cylinder; located it on the bottom; and recorded its final orientation, including the resting angle, and the elevation above the mudline. Additionally, cylinder heading was recorded by the divers using a small compass with storage memory.

In order to confirm the calculated trajectory of the cylinder, including the lateral travel from the point of release to its resting position on the seafloor, a small tethered metal weight

("stake") was also released just prior to the cylinder deployment. The divers then located the stake on the bottom and measured the distance from the stake to the cylinder and the compass heading of this direction to produce a complete set of data that allowed for the computation of the overall lateral travel of the cylinder. The ambient current profile was also measured using ADCP. Analysis of this data showed only minor lateral flows that were considered too small to influence the trajectory of the massive cylinder to any significant degree. Comparison of the diver measured and instrumentation processed data showed good agreement in all those deployments where reliable diver measurements were available.

The accurate determination of the dynamic parameters of the falling cylinder at the point of contact with the sediment was required for implementation of the predictive algorithm describing penetration into the mudfloor. The parameters required for input included two components of linear velocity, vertical and horizontal, pitch, and angular velocity in the vertical plane (plane of the mine) at the instant of initial contact with the sediment.

Experimental impact determination

Results of the analysis presented here are sensitive to the accurate determination of the actual initial contact of the mine body with the sediment. Selection of this point of impact can be done using two different methods. One is based on the diver observed elevation of the mine at rest, embedded in the sediment, and the other is based solely on the observed variations of various dynamic parameters of the mine as it is falling through the water and penetrating into the mud.

The first method utilizes the measurements of the maximum amount of mine exposed above the mean sediment floor level and incorporates the value of the orientation angle from the accelerometers. Accelerometers provide a very reliable measure of the inclination angles when stationary. We estimate that these measurements are more reliable than the diver measured pitch (at rest) taken using a hand-held inclinometer device (used in Cocodrie 2002 and Corpus Christi 2002 cruises). Knowing the final orientation and position of the cylinder embedded in the sediment, the initial point of contact of the body with the sediment floor can be back-calculated using the recorded values of local accelerations and angular rotation rates.

The second method of calculating the apparent initial contact of the falling cylinder with the sea floor is based solely on observation of the change in various quantities with time. The quantities of interest include the three components of linear acceleration (in either local or global coordinate system), total vector of global acceleration, or the angular rotation rates. One could plot the variation of these quantities with time and attempt to find the location of the sudden change in the rates of change of these variables as the cylinder comes in contact with the mud floor. This contact causes sudden deceleration and is also often associated with a sudden change in the variation of the angular rotation rates, as the mine body pivots about its nose as the translational movement is slowed, and if the penetration depth is such that a significant portion of the cylinder length is still protruding above the sediment floor. Cylinders tested here were nose-heavy, forcing the initial point of contact to occur in the frontal section.

There is a complication, however, associated with the choice of this initial contact point, when the second approach is used. The behavior of the cylinder, moving through the water, includes a "trapped water" effect, when a certain amount of fluid, immediately adjacent to the body, is participating in the motions of the cylinder. This volume of water generates a pressure front traveling in front of the body that "senses" the sediment before the actual contact with any part of the cylinder. The extent of this trapped water effect depends on the current orientation of

the cylinder, velocity, and rotation rates, as well as the geometry of the mine body. It was observed [6] that various nose shapes had an effect on the trajectory of the body. Blunt nose (in this nose heavy configuration) creates the largest pressure front, extending the farthest distance away from the mine, and the hemispherical one – the lowest. This trapped water effect sometimes complicates the manual determination of the initial contact with the sediment, as the rate of change of variables at certain orientations can be slow with no pronounced discontinuities. Penetration into softer sediments further complicates the problem, as the softer medium generates smaller resistance to the penetrating body, thus producing smaller changes in all the dynamic variables. A certain amount of engineering judgment had to be applied in these cases to determine the apparent instant of the initial contact of the cylinder with the mudfloor.

It was decided to utilize the first method, relying on the diver measured elevations to pick the time of contact of the cylinder with the seafloor. This method appears to the authors to be more self-consistent producing more reliable results especially in softer soil deposits.

Statistical description of the dynamics of impact burial

Performing a general statistical analysis of the dynamics of cylinder penetration into sediments may be useful in trying to identify the individual variations of various dynamic parameters. Patterns may be observed that could suggest alternative modeling decisions or provide a better understanding of the entire process of impact penetration of large cylindrical bodies into the soft cohesive marine sediments.

Fig. 4 through Fig. 7 show statistical description of variation in several dynamic parameters during sediment penetration process. Since the test series were performed at two different sites, direct comparison and analysis of behavior of each nose type is not always possible due to the limited number of deployments representing a similar configuration. Additional test results are currently being processed and, when completed, will improve the statistical descriptions of the dynamic processes. Several conclusions may, however, be drawn from analyzing these figures. Since significant scatter is present due to the varying orientations, velocities, and rotations on impact, the data, discussed hereafter, is only described in the mean sense.

It appears that the penetration events last no longer than 0.5 to 0.6 sec from the time of the initial contact with the sediment. There appears to be no significant difference between the two sites (G06 vs. P02), with respect to the vertical component of velocity (Fig. 4) or pitch (Fig. 5). The means are located close to each other with high variances, rather characteristic of the problem of free-fall dynamic penetration. Discrimination by the nose type, including hemispherical, blunt, and chamfered noses, is presented also and does not appear to result in any significant differences in behavior of the mean. The variance, however, appear to be dramatically higher for the chamfered nose, decreasing for the hemispherical one, and further decreasing for the blunt nose. This could in part be attributed to the more “erratic” behavior of these shapes due to the presence of inclined surfaces that may serve as guiding planes during the penetration event, dependent on the current orientation. Similar results were obtained by [6] characterizing the behavior of cylinders in free-fall through the water.

Variations in the rotational rate are presented in Fig. 6. Here, variation is observed between the two sites, as well as for the three different nose configurations. Higher rotational rates as well as the earlier peak were observed in the Cocodrie experiment (P02), and for the hemispherical configuration. Again, since only limited number of tests has been performed at the

two sites, both factors, nose shape and local sediment conditions, appear to be the contributing factors. There is no sufficient evidence, at this point, to differentiate between these two influences.

Time series of the cylinder penetration are shown in Fig. 7. It appears that the cylinders with the chamfered nose penetrate the most, on average, and the hemispherical – the least. This could be partially due to the fact that in the nose heavy configurations, as tested here, the hemispherical nose tends to change the direction of the overall momentum upon impact, redirecting it more in the horizontal direction, which results in decreased vertical penetration. Among the two sites tested, Corpus Christi location recorded deeper overall penetrations than Cocodrie. This could also be due to the somewhat higher strength at the Cocodrie site. Higher resistance to penetration would increase the angular rate more upon initial contact with the stronger sediment than with the softer sediment, producing results seen in Fig. 6.

We will now present the theoretical predictions and compare them with the experimental observations.

Experimental results and comparison with predictions

Mean vertical penetration of the cylinders is shown in Fig. 8 as time series. Comparing values in Fig. 7 with Fig. 8, one can observe that although the overall tendencies are correctly predicted, such as the higher penetration of the chamfered noses and the lowest of the hemispherical one, on average, the model over-predicts the amount of vertical penetration. The potential outcome of this prediction, in its impact on the Navy mine clearance operation, would be the fact that the threat in the area of interest would be overestimated. Given the actual values of the amount of mine protruding from the sediment, especially in the Corpus Christi case, the only decision that may be taken would be the decision of not entering the area of interest, as most mines would be expected to be buried below a typical detection limit.

Fig. 9 through Fig. 11 present a comparison of model predictions to the values measured experimentally for the three main parameters of interest – volume of the mine exposed, height protruding, and pitch at rest. Another parameter of interest, often used for analysis, *i.e.* surface area of the mine exposed, was found to be very similar in behavior to that of the amount of volume exposed and is, therefore, not presented herein for brevity. There is a fair amount of scatter in the experimental results, particularly noticeable in Fig. 9. Whereas in average, the model performs reasonably well, the variability of the data is quite significant, with individual predictions differing by as much as a factor of two to three from the measured values. These differences occur in both directions, over- or under-predicting the actually measured conditions. Additionally, it is noticeable that the model tends to overestimate the volume of mine buried, on average, as about twice as many points are located below the line of equality, as they are above.

Prediction in the maximum elevation of the mine, protruding from the sediment floor is shown in Fig. 10. It appears that most predictions are higher than their measured counterparts, for both of the testing sites, restating the facts presented earlier in Fig. 8. It is also interesting to note that almost all of the predicted pitch angles at rest, shown in Fig. 11, are higher than those measured. Only two of the 21 prediction points lie below he line of equality in this figure, suggesting that the angular momentum dissipation in the sediment is not accounted for accurately. These differences are not drastic, suggesting a reasonable approximation, but when combined with the predictions in the height exposed, lead to the overall underestimation, on average, of the volume exposed. It appears that the amount of rotation, occurring on impact, is

underestimated, which could be a potential source of error in the predictions of other parameters of interest, such as height and volume exposed. This phenomenon has been noted before [7] in preliminary comparisons of experimental data and model predictions.

The summary of the predictions versus the measured quantities is given in Fig. 12 and Fig. 13. The bar charts indicate the mean differences between predicted and measured values of the four variables shown on the x-axis. The two charts differentiate the data by site and by the nose configuration. Additionally, the calculated standard deviations are represented as error bars. High degree of variability is evident, especially in predicting the volume and area exposed.

There may be another source of errors in the predictive model, producing some of these discrepancies. The current model is two-dimensional requiring only four parameters for description (two linear and one angular velocity, and pitch angle), whereas the full three-dimensional description would require six components (3 linear and 2 rotational velocities, and pitch). In the next chapter we analyze the effects of the neglected degrees of freedom on the performance of the model.

Three-dimensional versus two-dimensional modeling of impact burial

An estimation of the relative influence of the neglected degrees of freedom on the overall predictions of the model could be done by observing the changes in a dynamic parameter that is not included in the model. One such parameter could be a linear velocity acting in the transverse or out-of-plane direction. Amount of kinetic energy dissipated during the cylinder motions through the sediment could be estimated using the following formula:

$$\int \left| V_{Y'} \right| dt \ .$$

The absolute value of the transverse velocity (Vy') represents a generalized measure of the energy dissipated in this direction. Plotting the absolute values of the differences between the model predictions and experimental observations versus this integral measure would have to show a progressive increase, if this missing degree of freedom contributes significantly to the overall predictions. These calculations are presented in Fig. 14, Fig. 15, and Fig. 16, depicting the primary three variables of interest – volume, height exposed and pitch at rest. A linear regression was performed and the correlation coefficient shown on each chart. It is obvious that the suggested correlations are only very weak at best. Fig. 14 show almost no correlation at all, meaning that the ability of the model to predict the amount of volume exposed is unaffected by the reduction to the 2-D configuration. The correlation coefficient in Fig. 15 is only marginally higher, indicating a similar situation in the prediction of the height protruding. The last figure of the series, Fig. 16, shows a weak correlation, suggesting that the dimensionality simplification implemented in the model has some, albeit very small effect on the predictions of the pitch angle. It would be advisory to add experimental data to this description, as it becomes available, to substantiate this observation. Based on the data presented here, only a minor improvement in the model predictions is expected by adding the third dimension to the formulation. It has to be concluded, therefore, that most of the inaccuracies in the model prediction, in its present formulation, comes probably from the material description itself, and not from the reduced dimensionality implemented in the code.

Discussion and conclusions

The paper presents results of two series of experimental deployments of a fully instrumented cylinder, deployed at two different locations in the Northern Gulf of Mexico. The paper focused on statistical description of the motion of a large cylindrical body through soft marine sediments. It was observed that the entire process of penetration, from the intial contact of the forward section of the cylinder with the mudfloor and until it comes to a full stop, embedded in the sediment, takes approximately 0.6 seconds. Analysis of individual dynamic parameters showed that there was little variation in the vertical component of velocity and pitch angle between the two sites explored or between the three different nose configurations employed. This conclusion was made by analyzing the time series of each of these parameters, in the mean sense. It was also observed that the variance in the distribution of these variables was the highest for the chamfered nose and the lowest for the blunt nose. It was argued that this could possibly be due to the effects of the chamfer as a guiding plane during the penetration events, as was also observed earlier [6], for the behavior of the cylinders free-falling through the water column.

Some differences were observed in the rotational rate, both between the two locations tested and the three nose types. Conclusive answers are somewhat difficult to make, at this point, since the amount of data currently processed is rather limited. Additional data will help separate the effects of the different soil profile at different locations and the varying nose shape. Similar conclusions were reached regarding the depth of penetration.

Comparisons between the experimentally measured and theoretically predicted values show that the model tends to under predict the volume and surface area of the cylinder exposed for all sites and all noses tested. Height protruding from the sediment was mostly overestimated, again for all locations and nose shapes. Pitch at rest was overestimated, somewhat significantly for all configurations tested. The overall predictions of the model were reasonable only in the mean sense. Individual comparisons of the measured versus the predicted values showed high variance and could either under- or over-estimate the measured parameters.

Examination of a hypothesis that neglecting the third dimension in the model formulations may result in some of the observed discrepancies was done utilizing a measure of kinetic energy dissipated in the transverse direction. The conclusion was reached, however, that the added dimensionality could only marginally affect the prediction in the pitch angle and is likely not be a contributing factor in improving the predictions for the volume or area exposed and height protruding from the sediment. It is the opinion of the authors, therefore, that any future improvements to the predictive model should focus on refining the physical model of the sediment, especially the strain rate effects during penetrations of large cylindrical objects into the soft mud floor.

Acknowledgments

This work is supported by the NRL Base Program, Project # BE-782-001, managed by Dr. Michael Richardson, Program Element No. 62435N. The Corpus Christi experiment was

supported by the Office of Naval Research Mine Burial Program, formerly managed by Dr. Roy Wilkens, now managed by Drs. Tom Drake and Brian Almquist, under PE# 62435N.

As any experimental study performed at sea, the success of this research would not be possible without the contributions of many people, including but not limited to C. Kennedy, C. King, C. Vaughn, G. Bower, M. Richardson, K. Briggs, R. Ray (all NRL), the captains and crews of R/V Pelican (Cocodrie) and R/V Gyre (Corpus Christi), and many others.

References

1. Chu, P.C., Gilles, A.F., Fan, C.W., Lan, J. and Fleischer, P., 2002. "Hydrodynamics of falling cylinder in water column." *Advances in Fluid Mechanics*, **4**, 163-181.
2. Kim, Y., Liu, Y., Yue, D.K.P. "Motion dynamics of three-dimensional bodies falling through water" (submitted).
3. Gilles, A.F., 1993. *Mine drop experiments (MIDEX)*, MSc thesis, Naval Postgraduate School, Monterey, CA.
4. Theophanis, S., 2002. "Accelerometer and Fiber Optic Gyro measurements of an Instrumented Cylinder used to study Impact Burial." *Proceedings of Oceans 2002 MTS/IEEE conference*, Biloxi, MS, October 29-31.
5. Holland, K.T., Green, A.W., Abelev, A.V., and Valent, P.J. "Parameterization of the in-water motions of falling cylinders using high-speed video" (in review) *Journal of Experiments in Fluids*.
6. Abelev, A.V., Valent, P.J, Plant, N.G., and Holland, K.T. (2003). "Evaluation and Quantification of Randomness in Free-fall Trajectories of Instrumented Cylinders." Proceedings, *Oceans 2003 marine technology and ocean science conference*, San Diego, CA, September 22-26 (DVD-ROM).
7. Valent, P.J., Dunlap W., and Abelev, A.V. (2003). "Mine impact burial prediction". Presentation at the 3rd annual ONR mine burial prediction workshop, St. Petersburg, FL, January 28-30.

Table 1. Cylinder configurations and initial conditions

#	Test name	Nose shape	Release medium	Height above water, m	Pitch at release, deg
Corpus Christi, TX, May 2002					
1	G06md02	hemi	water	-0.5	horiz
2	G06md03	blunt	water	-0.6	horiz
3	G06md04	blunt	water	-1.5	31
4	G06md05	blunt	air	0.5	horiz
5	G06md06	blunt	water	-0.8	horiz
6	G06md07	blunt	water	-0.8	horiz
7	G06md08	chamf	water	-0.6	horiz
8	G06md09	chamf	water	-0.8	horiz
9	G06md10	chamf	water	-0.6	horiz
10	G06md11	chamf	water	-0.6	horiz
Cocdrie, LA, January 2002					
11	P02md01	hemi	water	-0.5	horiz
12	P02md02	hemi	water	-0.5	horiz
13	P02md03	hemi	water	-0.5	31
14	P02md04	hemi	air	1	31
15	P02md05	hemi	air	0.5	31
16	P02md06	hemi	air	1	horiz
17	P02md07	hemi	air	0.2	horiz
18	P02md08	hemi	water	-0.5	horiz
19	P02md09	hemi	water	-0.5	31
20	P02md10	hemi	water	-0.5	31
21	P02md11	hemi	air	0.2	31

Notes: Pitch of 0 deg: long axis horizontal
Positive angles are nose down
Chamfered noses – released with chamf-up

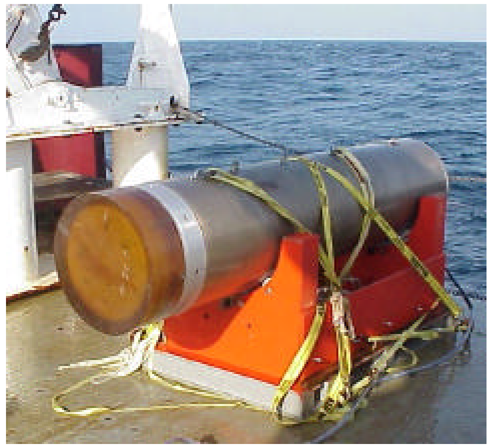

Fig. 1. General view of the instrumented cylinder with the blunt nose attached

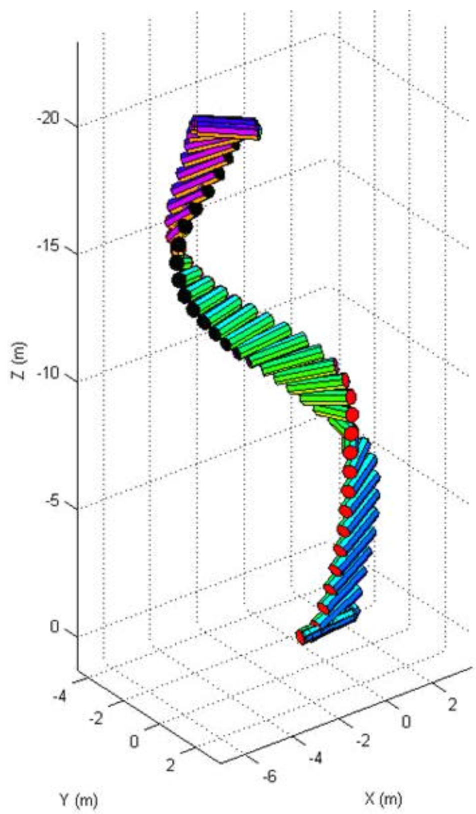

Fig. 2. A typical calculated trajectory of the instrumented cylinder in free-fall

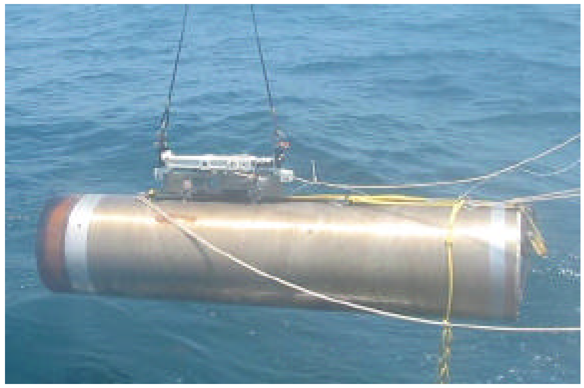

Fig. 3. Instrumented cylinder with the blunt nose attached, before an air release

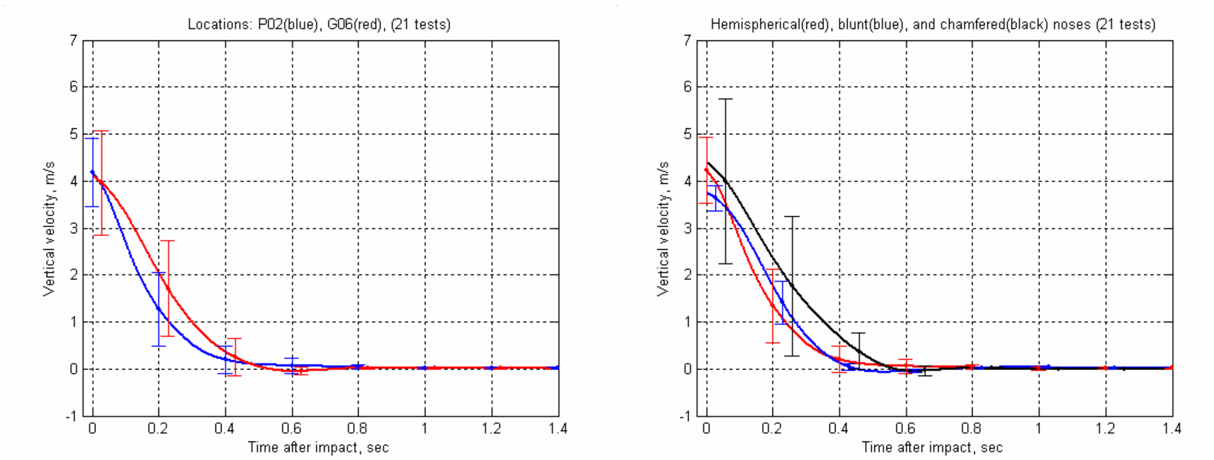

Fig. 4 Means and standard deviations of the vertical velocity, measured experimentally, distinguished by location and nose type

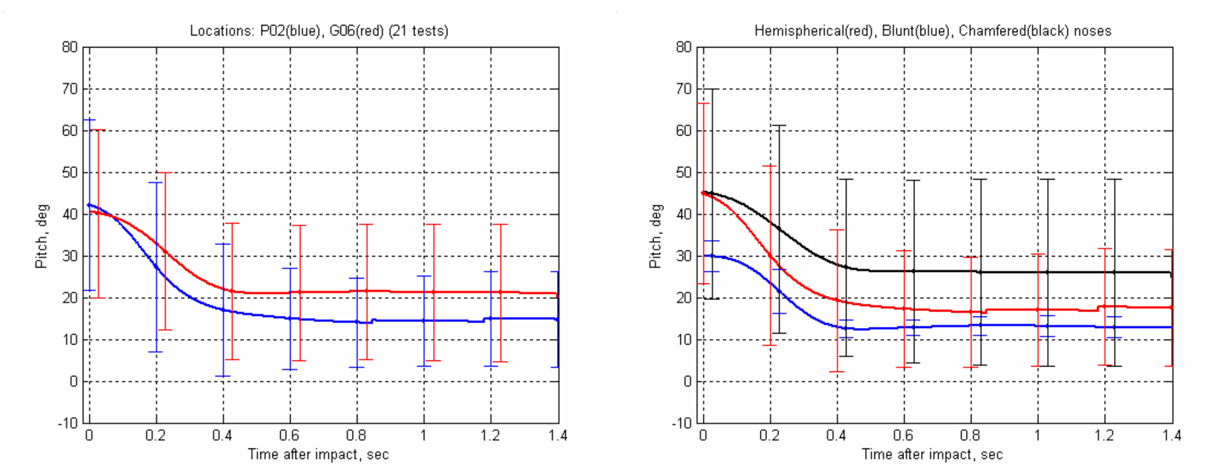

Fig. 5 Means and standard deviations of the pitch, measured experimentally, distinguished by location and nose type

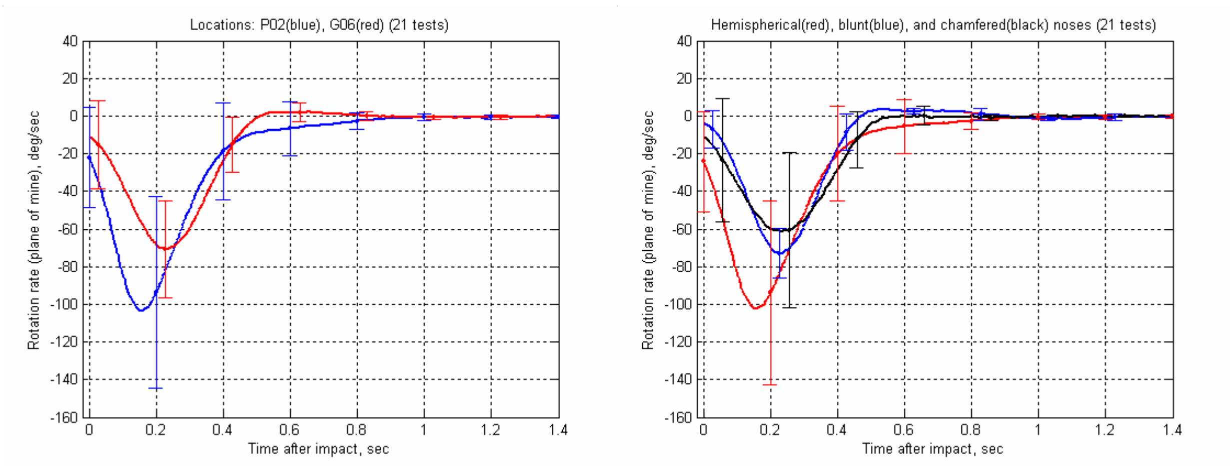

Fig. 6 Means and standard deviations the rotation rate, measured experimentally, distinguished by location and nose type

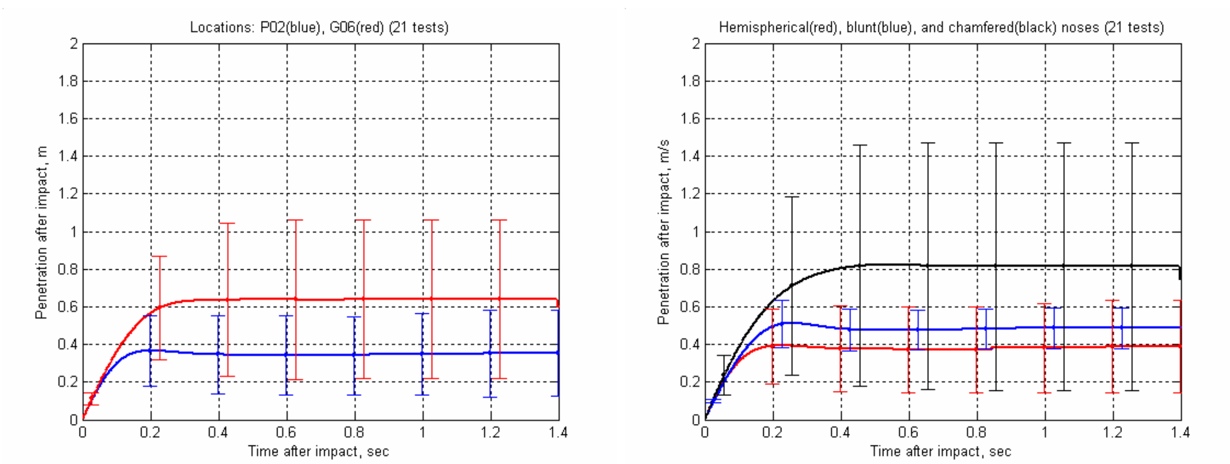

Fig. 7 Means and standard deviations of the penetration distance, measured experimentally, distinguished by location and nose type

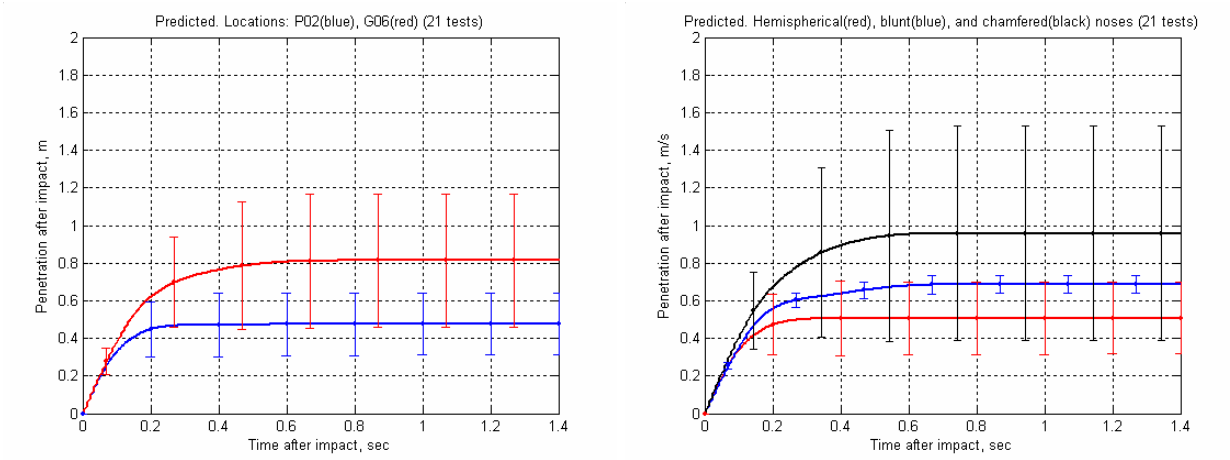

Fig. 8 Means and standard deviations of the penetration distance, predicted, distinguished by location and nose type

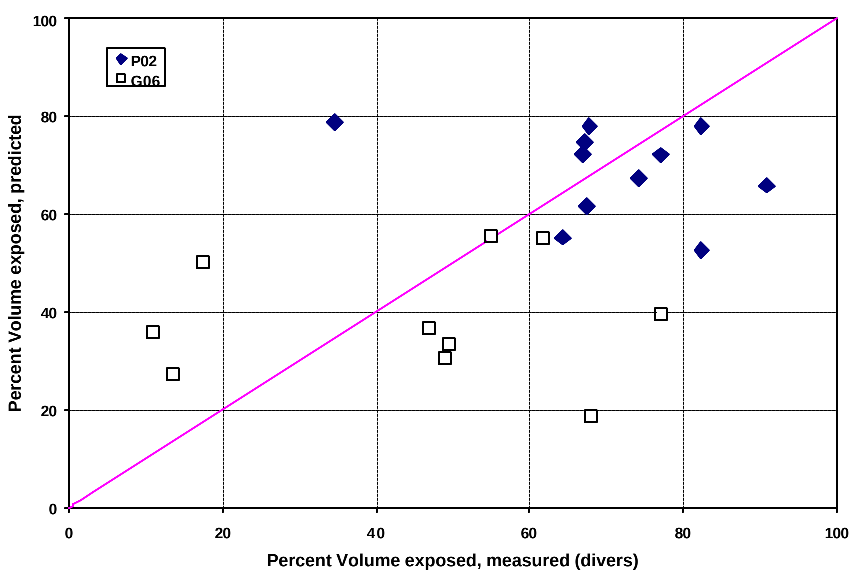

Fig. 9 Percent volume exposed at rest, predicted versus experimentally measured

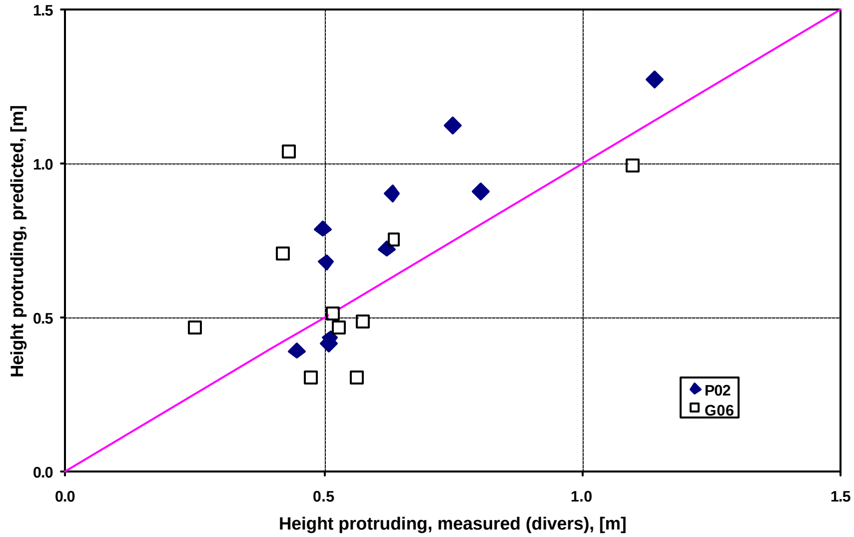

Fig. 10 Height protruding, predicted versus experimentally measured

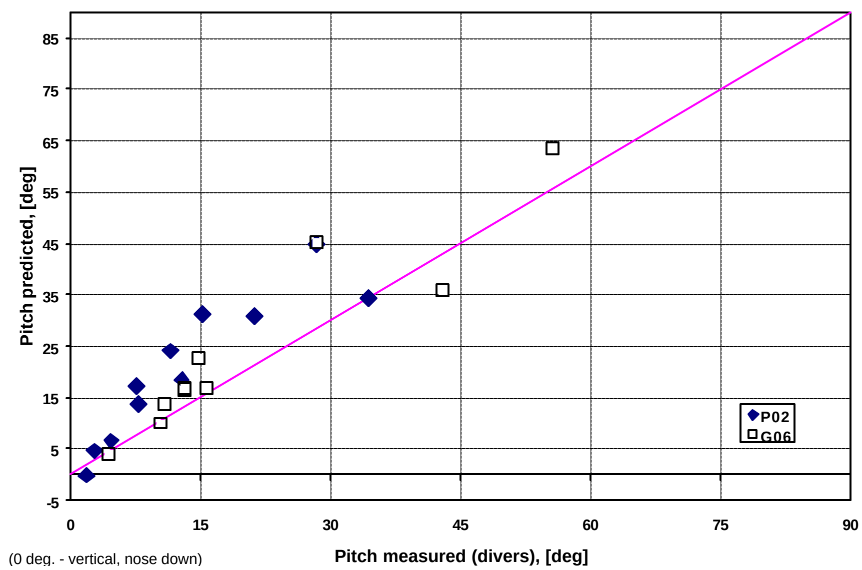

Fig. 11 Pitch, predicted versus experimentally measured

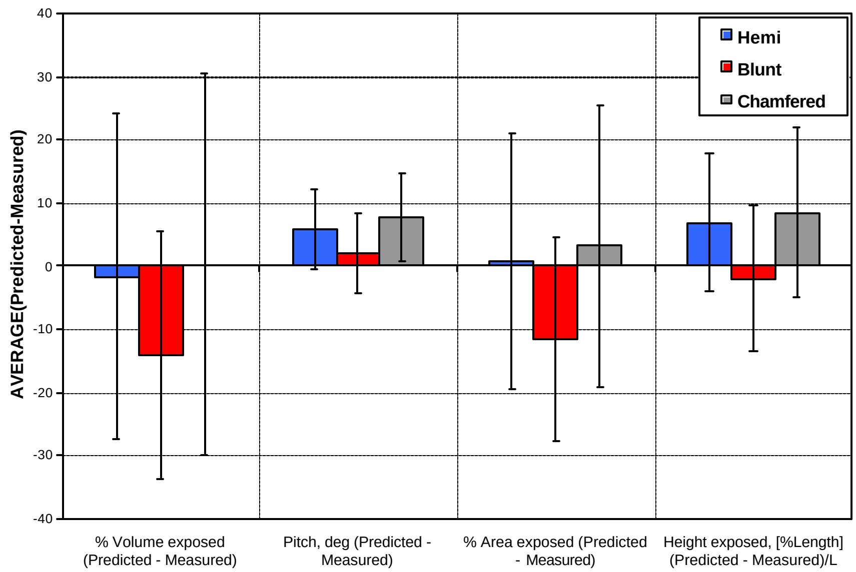

Fig. 12 Differences between measured and predicted variables, distinguished by the nose type

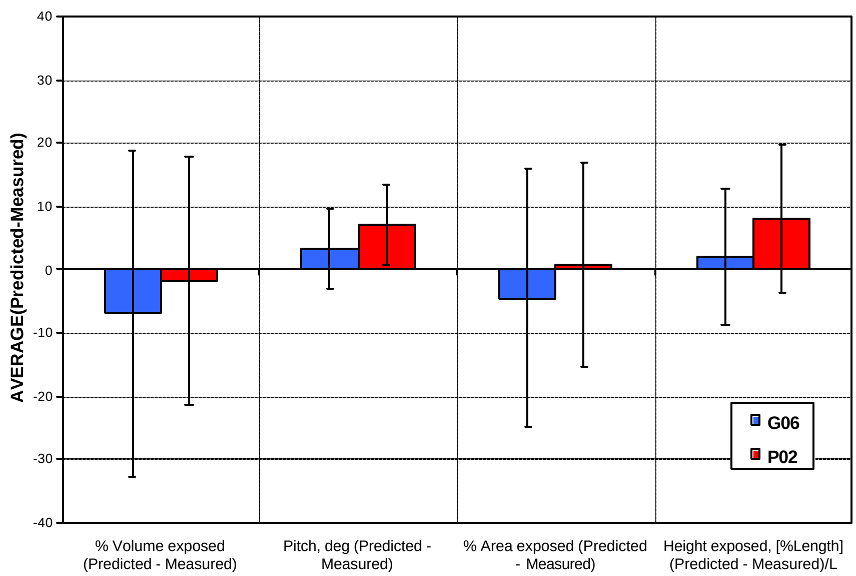

Fig. 13 Differences between measured and predicted variables, distinguished by the test location: G06 – Corpus Christi, TX, 2002, and P02 – Cocodrie, LA 2002

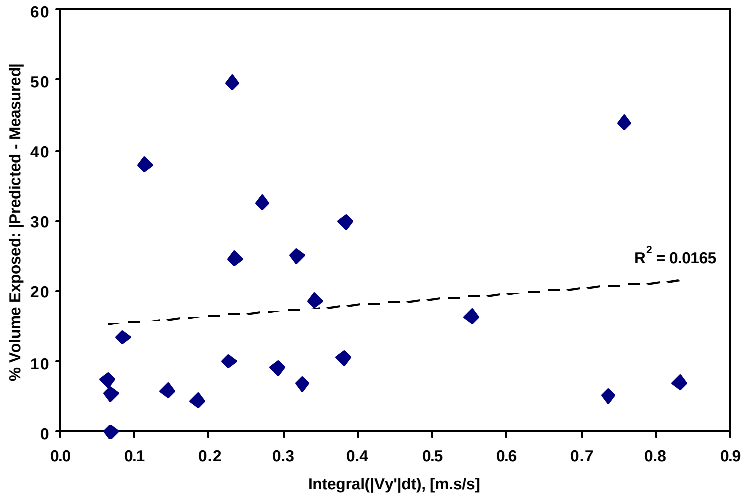

Fig. 14 The absolute difference between predicted and measured exposed volume versus the integral measure of transverse velocity component

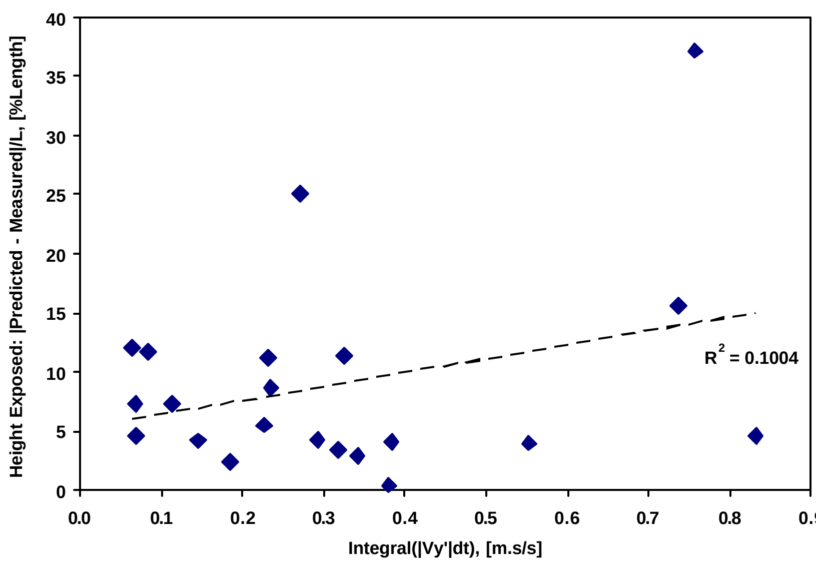

Fig. 15 The absolute difference between predicted and measured height protruding versus the integral measure of transverse velocity component

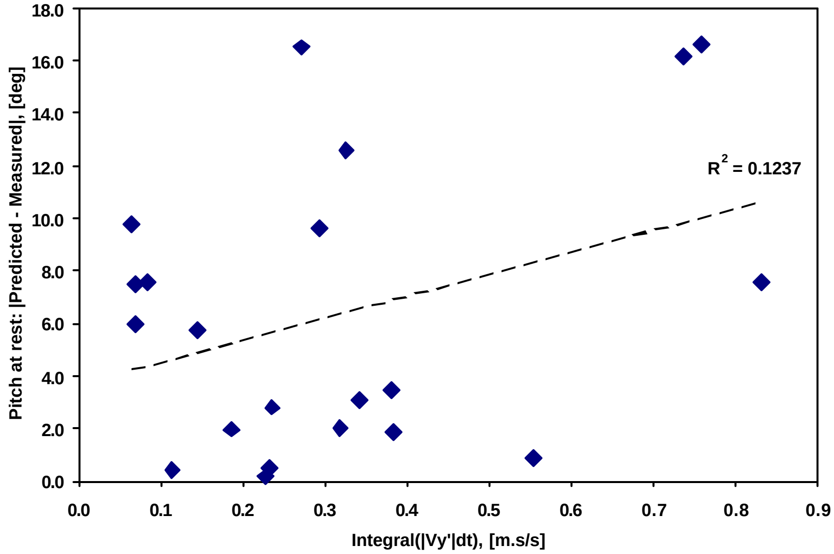

Fig. 16 The absolute difference between predicted and measured pitch at rest versus the integral measure of transverse velocity component